June 2009 *Volume 5 Issue 3*

Trade Science Inc.

Materials Science

An Indian Journal

Full Paper

MSAIJ, 5(3), 2009 [201-208]

Measurements of electron temperature and ion density in an AC pulsed oxygen plasma study

H.Martínez[1], F.B.Yousif[2]*, F.Castillo[3]

[1]Instituto de Ciencias Físicas, Universidad Nacional Autónoma de México, Apartado Postal 48-3, 62210, Cuernavaca, Morelos, (MÉXICO)

[2]Facultad de Ciencias, Universidad Autónoma del Estado de Morelos (UAEM), Cuernavaca, Morelos, (MÉXICO)

[3]Instituto de Ciencias Nucleares, Universidad Nacional Autónoma de Mexico, (MÉXICO)

E-mail : fbyousif@servm.fc.uaem.mx

Received: 13th May, 2009 ; Accepted: 18th May, 2009

ABSTRACT

Emission spectroscopy was employed to observe O_2 plasma generated by an AC discharge at pressures from 0.15 to 0.5 Torr. The emission bands and lines show linear dependence over the entire pressure range. Electron temperature measurements were performed using a double Langmuir probe. Measured electron temperature was found to be inversely proportional to pressure. Within the plasma conditions under consideration, O2, O_2^+, O, and O^+ play a dominant role in the pulsed plasma process within the spectral range of (200-800 nm), and the importance of these components vary little under the conditions of the plasma studied in this work. Identification of the vibrational levels of the $\mathbf{B}^3\Sigma_u^-$ excited state indicates that predissociation through a repulsive states coupling with the $\mathbf{B}^3\Sigma_u^-$ state may be responsible for the depletion of upper vibrational levels of this state.

KEYWORDS

Optical emission spectroscopy;
Pulsed plasma;
Glow discharge.

1. INTRODUCTION

Low-pressure plasma discharges in electronegative gases are widely used in modern plasma technology, primarily in microelectronics as reactors of plasma chemical etching and deposition of thin films. The elaboration of electronic components and structures of submicronic and smaller scale requires creation of highly effective, well controlled plasma reactors which cannot be created without a complete knowledge of the processes and phenomena taking place in them. It provides greater interest to researchers of both plasma chemical reactions and electrodynamics in electronegative gases. The discharge electrodynamics often turns out to be strongly connected with processes within the plasma. Substantial improvements of different characteristics of plasma-activated reactors have been achieved[1-8]. Varying power input and other characteristics of a pulsed discharge mode allows one to control rather easily the different plasma parameters.

Low-pressure plasmas have been studied in analytical spectroscopy as an excitation source for emission spectroscopy[9-11], with the advantage of less spectral interference. As the ionization and excitation of spe-

cies heavier than electron is related to electron collisions, the electron temperature (T_e) that represents the kinetic energy distribution of free electrons and the ion density (n_i), are the most important fundamental parameters for characterization of the plasma discharge. Within the pressure range of this work (less than 0.5 Torr), the collisional frequencies between electrons and atomic and molecular species is low, therefore local thermo dynamical equilibrium cannot be achieved. Consequently, electron temperatures higher than that of the heavier species are a characteristic that is observed. As a result, the electron temperature (T_e), and ion density (n_i) are essential parameters for the understanding of plasma parameters.

In this article, we report measurements made for electron temperature, and ion density in an AC pulsed Oxygen plasma employing double Langmuir probe and emission spectroscopy. The dependencies of these quantities on gas pressure and input power are presented and discussed.

2. EXPERIMENTAL

The experimental apparatus and technique to generate the pulsed plasma was recently reported[12,13]. A brief description is reported here. The system consists of two stainless steel circular plane electrodes, 1 mm thick and 50 mm in diameter. The electrodes are positioned at the center of the reaction chamber with 25 mm gap spacing. The gas was introduced into the reaction chamber through the upper flange. The same gas connection was used for the pressure sensor (MKS, Type 270 signal conditioner and 690A11TRC MKS Baratron). An AC, 60 Hz discharges was used to generate the plasma in O_2 gas. Ultra pure O_2 gases (Praxair 99.99%) were used in the course of the measurements. A quartz window was installed on the right lateral flange through which glow discharges were monitored by plasma emission spectroscopy. In front of this quartz window, a 200 mm of focal distance quartz lens (diameter of 25.4 mm) was positioned and the plasma emission was focused and collected through an optical fiber (Solarization-resistant UV and fiber diameter size of 400 μm) that was connected to the entrance aperture of a moderate-resolution Ocean Optics Inc. spectrometer Model HR2000CG-UV-NIR which has a spectral range of 200 to 1100 nm, equipped with a 300 lines-mm^{-1} composite blaze grating and a UV2/OFLV-5 detector (2048-element linear silicon CCD array). The grating response has a spectra response in the range of 300-1100 nm with efficiency > 30 %. The inlet and outlet slits were 5 μm wide. The data were obtained in a single accumulation of 10 s integration times, which corresponds to 600 times that of the period of the pulsed voltage. The wavelength scan interval was of 0.47 nm. The lens and fiber optics assembly were positioned to collect the emitted light appearing on the monomer surface and plasma. The pulsed plasma was produced in O_2 gas environment at pressures between 0.15 and 0.50 Torr. The discharge power supply was maintained at an output of 350 Volts and a current of 0.10 A (35 W), which was measured using a digital Tektronix multimeter model DM2510. The base pressure of the plasma chamber of 6.3×10^{-3} m^3 volume was 7.5×10^{-3} Torr (measured with a Thermovac sensor TR211 connected to a Thermovac TM20 digital controller), achieved using a mechanical pump (Trivac D10, Leybold Pump with nominal pumping speed of 11.8 m^3 h^{-1}). The vacuum chamber was purged with the working gas several times at a pressure of 1.0 Torr in order to remove the background gas.

2.1. Double langmuir probe

Langmuir probes are commonly used as a diagnostic tool for the determination of plasma parameters. The double probes were initially reported in the 1970s. Basically the Langmuir probe consists of one or two electrodes inserted into the plasma. In the double probe configuration, the current collected by the electrodes is measured as a function of the voltage applied between the two electrodes. From the current-voltage characteristics of the probe, electron temperature (T_e) can be derived. The double Langmuir probe employed in this work consists of a 0.0635-mm-radius tungsten wire (W-WI-005, Kimball Physics Inc.). The probe was located inside a glass capillary, having a hole of 0.7 mm diameter; inside the capillary, both wires were shielded separately with plastic insulating cylinders. The wire tips were extended 1.0 mm beyond the glass capillary to form the probe. The inside bore of the glass capillary was enlarged at the probe end, to form a cavity in order to prevent metal deposits on the glass, thus increasing

the probe area[14]. The probe was aligned parallel to the cylindrical axis of the discharge tube and could be moved only in the forwards and backwards directions in the center of the plasma by using a manual micrometer motion feed through.

The voltage difference applied to the probe was manually scanned from +30 V to -30 V and vice versa by a regulated dc power supply (EXTECH, Model 382213). The probe current was monitored by an Electrometer (EM, Model E16). The scanning time for one I-V curve was 5-10 minutes. Owing to sputtering or contamination of the probe tips, the total measurement time for one probe was restricted to approximately 5-6 h. The final I-V curves obtained were the results of an average of 6 data scans at each probe voltage.

3. RESULTS AND DISCUSSION

3.1. Characterization of glow AC discharge

The derivation of plasma parameters is based on a theoretical description of the double Langmuir probe current-voltage characterization. Usually, a distinction is made between the thin sheath limit (TSL) and the orbital motion limit (OML) regimens[15,16]. In the TSL, the plasma sheath, which is characterized by the Debye length

$$\lambda_D = \left[\frac{\varepsilon_0 k T_e}{e^2 n_e}\right]^{1/2} \quad (1)$$

is small relative to the probe dimensions (ε_0 is the permitivity of free space, T_e is the electron temperature, n_e, the electron density, k, Boltzmann's constant, ande, the electron charge). In this case, the probe current (I) as a function of voltage (V) is given[15,16] by

$$I = I_\infty \tanh\left(\frac{eV}{2kT_e}\right) \quad (2)$$

With the saturation current ($I\infty$) being dependent on ion density (n_i), oxygen ion mass (m_i= 16αmu), electron temperature (T_e) and probe area (A) as follows:

$$I_\infty = Aen_i\left(\frac{kT_e}{2\pi m_i}\right)^{1/2} \quad (3)$$

The second derivate of equation (2) exhibits two extrema. They are separated by a voltage difference ΔV, which can be used to calculate the electron temperature T_e[17]:

$$k_B T_e = \frac{e\Delta V}{\ln\left[(2+\sqrt{3})/(2-\sqrt{3})\right]} \quad (4)$$

However, frequently the probe is not working in the TSL. Therefore the ion 'saturation' current would increase as the voltage is increased. Nevertheless, the electron temperature obtained in this method is still valid in the non-TLS regime, since an increase in ion saturation current does not substantially change the location of the extrema in the second derivative. Thus in the worst case, using the TSL results for the OML, would result in an error of about 5%.

The evaluation algorithm runs in the following way. First the probe characteristic curve is differentiated two times and smoothed. Smoothing was performed by the procedure described by Savitzky and Golay[18]. The obtained current-voltage characteristic data for a 60 Hz generator that delivered a maximum of 35 W of power to the O_2 plasma at 0.30 Torr of pressure is displayed in figure 2. From the position of the extrema in the second derivative of the characteristics curve (dotted line in figure 2), the electron temperature is calculated using equation (4). Then a theoretical curve is fitted to the entire measured experimental current-voltage characteristic curve as given by equation (2) by adjusting only the ion density (n_i). This evaluation procedure gave an electron temperature of T_e=1.13 eV and an ion density of ni=1.98×10^{10} cm^{-3} (using n_e=n_i). In this case, the Debye length of λ_D=5.62×10^{-3} is small compared to the probe radius of 0.0635 mm, a condition that is called the transition region TSL. With a correlation coefficient of 0.987, figure 2 shows that the theoretical curve (solid line) fits very well to the mea-

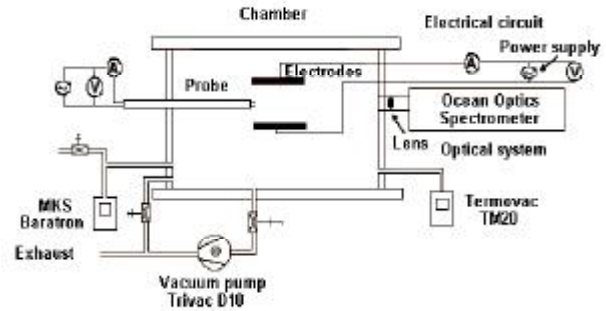

Figure 1: Schematic diagram of the experimental apparatus

Full Paper

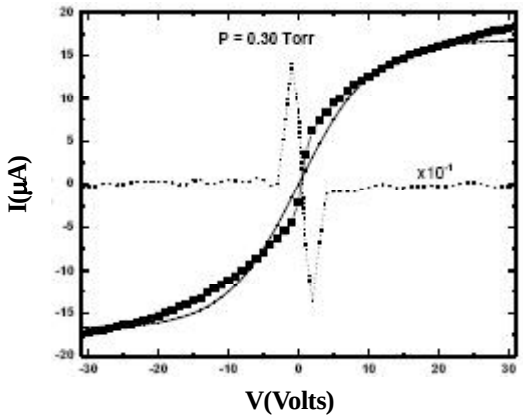

Figure 2: Double probe characteristic with second derivate (dotted line) and theoretical fit (full line)

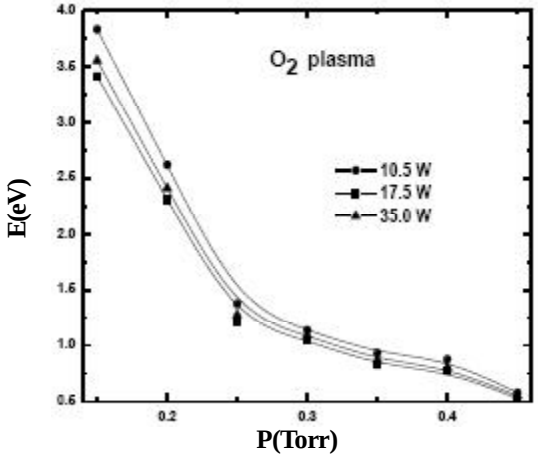

Figure 3: The electron temperature as a function of pressure obtained with the double Langmuir probe at three different operating powers

sured data.

Shown in figure 3, is the electron temperature as a function of pressure for three constant powers of 10.5, 17.5 and 35.0 W. The electron temperature is found to be inversely proportional to the pressure. The high electron temperature for lower pressures is typical of plasma discharges. At low pressures, the electron temperature must increase in order to sustain the discharge since a decrease in the neutral density results in lower ionization rate, while a pressure increase brings about a higher colliding frequency and thus a reduction in electron energy.

However electronegative ion density has been observed in both DC discharge and discharge afterglow plasmas[19,20] such as O_2 plasma. As a result it is expected that negative ion concentration to influence measured values of ion density and temperature. A qualitative description of the dynamics of negative ions in the active phase was introduced[19,20], namely the inclusion of the electron attachment to the $O_2(A^3\Sigma_u^+, A'^3\Delta_u, c^1\Sigma_u^-)$ metastable molecules. The destruction of negative ions in the discharge by detachment process, essentially influence their dynamics. Yet, discrepancy was observed in absolute value between the calculated and measured concentration of negative ions as well as temperature and density of electrons. Ivanov et al.[19] studied the spatial structure and dynamics of a pulsed dc discharge in oxygen plasma as well as the effect of different electron attachment processes on the dynamics of the negative ion density. It was shown that in the discharge, the main production mechanism of negative ions was the dissociative attachment of slow electrons to metastable oxygen molecules $O_2(A^3\Sigma_u^+, A'^3\Delta_u, c^1\Sigma_u^-)$. This was possible since the pulsed discharge at low pressure in[20] has a spatial structure providing the effective generation of fast electrons in the cathode sheath. Such quasi beam of running a way electrons degrade in the area of a low electric field by providing an accumulation of slow electrons. Therefore the electron energy distribution function in the plasma volume appears to be nonlocal. Ivanov et al.[19] found that the discharge dynamics is essentially non-stationary. During the discharge pulse, there was an accumulation of charged particles and excited molecules in the bulk of the plasma. The density of the negative ions in the discharge was determined by the balance between their production at the attachment of the slow electrons to highly excited oxygen molecules in the Herrzberg's states $A^3\Sigma_u^+$, $A'^3\Delta_u$, $c^1\Sigma_u^-$ and their destruction in collisions with metastable molecules O2($\alpha^1\Delta_g$). As a result, the accumulation of excited oxygen molecules plays the main role in the production of negative ions in low-pressure oxygen pulsed discharge. Ivanov et al[19] has shown that the ratio of negative ions to those of electrons was 0.2 for both measured and calculated values[20]. This would imply that the electonegativity of the oxygen plasma is expected to lower the true value of positive ions and electron density by 20% . Lichtenberg et al[20] developed a macroscopic analytic model for three component electronegative plasma. This model was designed to pre-

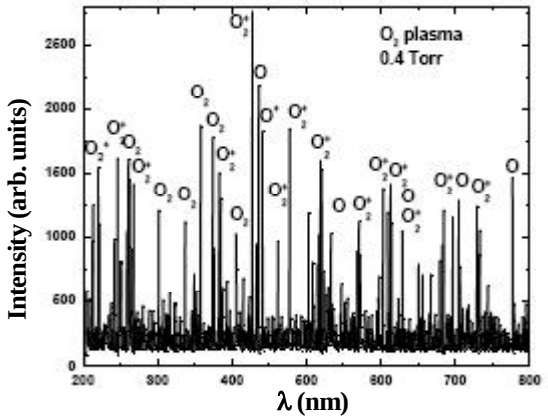

Figure 4: Emission spectra of O_2 plasma at 0.4 Torr and 17.5 W

dict values of plasma quantities such as electron and negative ion densities and electron temperature as the neutral pressure and power to the plasma were varied. Their[20] results shows that at the minimum of plasma length to the sheath edge, the ratio of n_-/n_e was >1. This ratio decreased as the plasma length to the sheath edge was increased reaching unity as that distance was just below the mid-point between the two electrodes. At the mid point between the two electrodes, the ratio n_-/n_e becomes very small and $n_e=n_+$ as reported in[20] indicating that as plasma length to the sheath edge increases beyond this point, the electrons dominate the plasma.

Since in our experimental work, the probe position was at the mid-point between the two electrodes, therefore it is safe to assume at that point (mid-point between electrodes) our measured positive ion density would correspond to the electron density[20]. As a result it can be stated qualitatively that for electronegative plasma such that of oxygen, at small plasma length to the sheath edge, the negative ions influence the measurements of the electron density rather severely. That effect decreases as the probe is moved a way from one electrode toward the second electrode, and electrons dominate the plasma at plasma length to the sheath edge just below the mid-point between the two plates.

3.2. Emission spectrometry measurements

A typical spectroscopic emission measurement of O_2 glow discharge plasma at a pressure of 0.40 Torr is displayed in figure 4 at 35.0 W of power. This allowed analysis of the most luminous area, which corresponds to the negative glow near the cathode dark space. Identified species in the spectra of figure 4 are reported in TABLE 1. Although the spectral range of the spectrometer is that between 200 and 1100 nm, yet no emission lines were observed above 800 nm. Therefore only the most intense spectral bands and lines of O_2, O_2^+, O and O^+ within the 200-800 nm range are quoted[21]. The observed peaks centered at 261.3, 337.0, 358.2, 374.3 and 429.4 nm corresponds to the most intense peaks of the $O_2(B^3\Sigma_u^- - X^3\Sigma_g^-)$ transitions, while the broad band with a maximum at 300.2 and 406.4 nm corresponds to the most intense peaks of the

TABLE 1: Summary of emission spectra observed in O_2 discharge within the wavelength of 200-800 nm

Emission species	Electronic transition	ν′	ν″	Wavelength (nm)
				436.8
				533.1
O (Atomic line)				615.6
				700.2
				777.2
O^+ (Atomic line)				442.5
		1	8	261.3
		0	14	337.0
O_2	$B^3\Sigma_u^- \rightarrow X^3\Sigma_g^-$	1	16	358.2
		1	17	374.3
		1	20	429.4
		4	5	300.2
O_2	$A^3\Sigma_u^+ \rightarrow X^3\Sigma_g^-$	0	7	406.4
		3	1	527.5
		0	0	602.6
		1	2	635.1
O_2^+	$b^4\Sigma_u^- \rightarrow a^4\Pi_u$	0	2	685.6
		1	4	723.5
		0	3	733.5
		12	1	213.9
		9	1	221.4
		5	2	246.5
		5	3	259.4
		4	3	263.3
		6	4	266.7
		0	8*i*	383.5
O_2^+	$A^2\Pi_u \rightarrow X^2\Pi_g$	0	8*ii*	386.0
		0	9	411.6
		0	11	467.9
		1	12	482.0
		0	12	503.5
		0	12	508.6
		1	14	567.8
		1	15	610.3

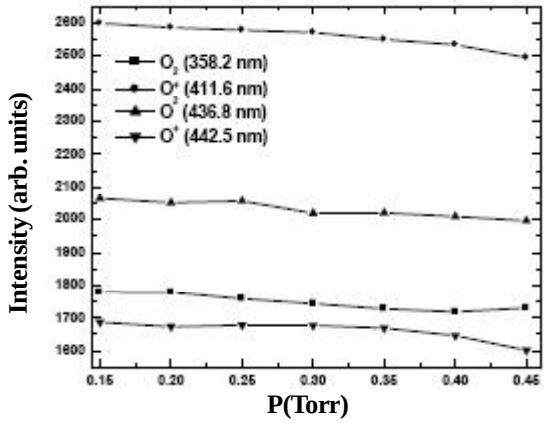

Figure 5: Emission intensities as a function of pressure

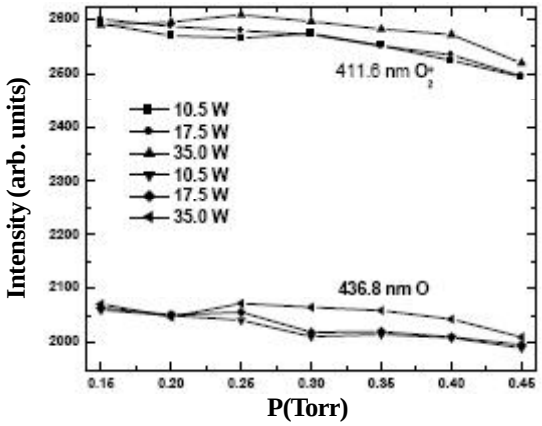

Figure 6: Emission intensities as a function of pressure and power discharge

$O_2(A^3\Sigma_u^+ - X^3\Sigma_g^-)$ transitions. The observed peaks at 527.5, 602.6, 635.1, 685.6, 723.5 and 733.5 nm corresponds to the most intense peaks of the $O_2^+(b^4\Sigma_u^- - a^4\Pi_u)$ transitions, and the broad band with a maximum at 300.2 and 406.4 nm correspond to the most intense peaks of the $O_2^+(A^2\Pi_u - X^2\Pi_g)$ transitions. The observed peaks at 436.8, 533.1, 615.6, 700.2 and 777.2 nm were assigned to the strong lines of atomic Oxygen**.** Finally, the peak at 442.5 nm corresponds to the O^+ atomic line.

The pressure dependence, of several emission bands and lines at 358.2 nm for O_2; 411.6 nm for O^+_2; 436.8 nm for O and 442.5 nm for O^+, is shown in figure 5. Linearity of this dependence is observed with line intensity remaining nearly constant within a pressure range of 0.15 to 0.45 Torr. Figure 6 displays the emission intensities as a function of pressure at different values of injected power between 10.5 and 35 W for the O^+ at 411.6 nm, and 436.8 nm for atomic Oxygen**.** A constant dependence of line intensities is observed as a function of power. It can be seen that for both lines, the intensity show negligible dependence on power.

Considering the plasma conditions, it can be inferred that excited O_2, O_2^+, O^+ and O plays an important role in the pulsed plasma process within the wavelength range of 200-800 nm. The importance of these components in the pulsed plasma process vary little under the conditions of the plasma studied in this work. This fact may not apply to regions outside the above mentioned spectrometer range on one hand, while on the other hand, other techniques such as Actinometry, or laser laser induced fluorescence may also be of importance in defining the evolution of the molecular/atomic/ionic density as a function of pressure or power.

From the parent gas O_2, excited neutral molecules as well as the primary radicals O and O^+, and O_2^+ in their ground and excited states, are generated during each pulse by electron impact as follows:

$$O_2 + e \rightarrow O_2^* + e$$

$$O_2 + e \rightarrow O + O + e$$

$$O_2 + e \rightarrow O^+ + O + e + e$$

and

$$O + O \rightarrow O_2$$

In turn, the O_3 may undergo the following reactions with O:

$O_3 + O \rightarrow O_2 + O_2$, While the O may react with another O resulting in the formation of O_2 and O_2^+. On the other hand may experience further vibrational excitation in collisions with electrons.

Interplay between formation and destruction processes is rather complicated depending on many parameters and a full kinetic model is required in order to get a deeper insight in understanding the mechanisms resulting in the formation of O,O+,O2 and O^+_2. Within the experimental parameters of the plasma studied in this work, the plasma generated under each parameters of power and pressure reach an equilibrium at which the above-mentioned radicals are the dominant species.

The emission spectra shown in figure 4 identify the

upper states involved in the emission lines and bands to be of O, O^+, and O_{2B} $O_2(B^3\Sigma_u^-)$, $O_2(A^3\Sigma_u^+)$, $O_2^+(b^4\Sigma_u^-)$ and $O_2^+(A^2\Pi_u)$ in specific vibrational levels as listed in TABLE 1. The following analysis with the aid of the potential energy curves for O_2, and O_2^+[22] is presented in order to understand why these specific vibrational levels listed in table I, are responsible for the emission lines and bands observed in the spectra of figure 4. Since the O_2 ground state and the excited state O_2 $(B^3\Sigma^-_u)$ have their minima at 1.2 and 1.6 Å[23], therefore it is expected that excitation in the Frank Condon region would result in most of the upper vibrational levels of the O_2 $(B^3\Sigma^-_u)$ state to be populated. Yet as seen in table I, the population of the O_2 $(B^3\Sigma^-_u)$ is mostly at ν=0 and 1, and no emission bands were observed resulting from O_2 $(B^3\Sigma^-_u)$, with ν>1. The absence these emission lines and bands can be explained in terms of the coupling of O_2 $(B^3\Sigma^-_u)$ with repulsive dissociative states such as $^3\Pi_u$ and $^1\Pi_u$.

The O_2 $(B^3\Sigma^-_u)$ is crossed by repulsive curves such as $^3\Pi_u$ and $^1\Pi_u$. The coupling of these states with the O_2 $(B^3\Sigma^-_u)$ at vibrational levels higher than ν=1, would result in the predissociation of this state leading to $O(^3P)+O(^3P)$. Similarly, the $A^3\Pi_u^+$ which has the minima of its potential well just below1.5Å, therefore it can be populated mostly in its upper vibrational levels since the excitation of the $X^3\Pi_g^+$ occur in the frank Condon region at around 1.2Å. This is reflected in the observed emission band.

On the other hand, with respect to the emission band resulting from $A^3\Pi_u \rightarrow X^2\Pi_g$, the $A^3\Pi_u$ has its potential minima around 1.4 Å, implying that excitation in the frank Condon region would result in populating most of the vibrational levels of the $A^3\Pi_u$ state with the probability of the lower vibrational levels populated to smaller. This can be seen from the observed emission bands and lines tabulated in TABLE 1.

CONCLUSIONS

Electrical and optical characterization of a pulsed plasma discharge study of Electrical and optical characterization of a pulsed plasma discharge study of O_2 gas is presented. The emission from the pulsed plasma of a steady-state electric discharge in O_2 at total pressure within the range of 0.1 to 0.5 Torr, was investigated in the wavelength range 200-800 nm. Electron temperature was found to be inversely proportional to the pressure. Within the pulsed plasma conditions, and within the spectrometer range of 200-1100 nm, it was observed that excited O2, O_2^+, O^+, and O play a dominant. The emission consists of $O_2(B^3\Sigma_u^- - X^3\Sigma_g^-)$, $O_2(A^3\Sigma_u^+ - X^3\Sigma_g^-)$, $O_2^+(b^4\Sigma_u^- - a^4\Pi_u)$, $O_2^+(b^4\Sigma_u^- - a^4\Pi_u)$ and $O_2^+(A^2\Pi_u - X^2\Pi_g)$ transitions. Emission bands resulting from $O_2(B^3\Sigma_u^-)$ excited state in ν=0 and 1 only were observed, probably due to the coupling of the $O_2(B^3\Sigma_u^-)$ state with a repulsive predissociative states such as $^3\Pi_u$ and $^1\Pi_u$, resulting in the depletion of the vibrational levels (ν>1) via predissociation resulting in O atoms. Similar explanations apply with respect to $A^3\Sigma^+_u$, while for the $A^2\Pi_u$ excited state with potential minima at around 1.4Å, the probability for excitation from the $A^2\Pi_g$ is to most of the vibrational levels of the $A^2\Pi_u$ state. Spectral lines and bands intensities were shown to have linear dependency on discharge pressure in the range of 0.15 to 0.5 Torr. Also a constant dependence of lines and bands intensities is observed as a function of power.

ACKNOWLEDGMENTS

The authors are grateful to Armando Bustos, Anselmo González, and José Rangel for technical assistance. This research was partially sponsored by DGAPA IN-105707-3, CONACyT 41072-F and CONACyT 43643/A-1.

REFERENCES

[1] P.N.Guzdar, A.S.Shiratani, S.K.Guhary; Appl.Phys. Lett., **71**, 3302-3304 **(1997)**.

[2] W.Watanabe, M.Shiratani, H.Makino; Appl.Phys. Lett., **57**, 16165-1618 **(1990)**.

[3] W.Watanabe, M.Shiratani, Y.Kubo, I.Ogawa, S. Ogi; Appl.Phys.Lett., **53**, 1263-1265 **(1988)**.

[4] L.J.Overzet, J.T.Verdeyen; Appl.Phys.Lett., **48**, 695-697 **(1986)**.

[5] M.Shiratani, T.Fukuzawa, E.Eto, Y.Watanabe; J. Appl.Phys., **31**, L1791 **(1992)**.

[6] W.X.Ding, L.A.Pinnaduwage, C.Tav, D.L. McCorkle; Plasma Sources, Sci.Tecnol., **8**, 384-391 **(1999)**.
[7] A.A.Kudryavtsev, L.D.Tsendin; Tec.Phys.Lett., **26(7)**, 582-587 **(2000)**.
[8] A.A.Kudryavtsev, A.L.Kuranov, V.G.Mishakov, T.L.Thahenko, I.N.Skoblo, M.O.Chayka; J.Tech. Phys., **46(3)**, 299-306 **(2001)**.
[9] D.C.Miller, C.J.Seliskar, D.M.Davidson; Spectrosc., **39**, 13 **(1985)**.
[10] J.Lim, J.Kim, C.Lee, G.Back, Y.Lee; Spectrosc. **54**, 1253 **(2000)**.
[11] Y.Sung, H.B.Lim; J.Anal.At.Spectrosc, **16**, 767 **(2001)**.
[12] H.Martínez, B.F.Yousif, A.Robledo-Martínez, F. Castillo; IEEE Transactions on Plasma Science, **34(4)**, 1497-1501 **(2006)**.
[13] H.Martínez, A.Rodríguez-Lazcano; Plasma Source Science and Technology, **103(4)**, 2591-2596 **(2007)**.
[14] J.A.Thornto; J.Vac.Sci.Technol., **15**, 188 **(1978)**.
[15] J.D.Swift, J.R.Schwar; Electric Probes for Plasma Diagnostics, New York, Elsevier.
[16] A.Brockhaus, C.Brochhardt, J.Engemenn; Plasma Sources Science and Technology, **3**, 539 **(1994)**.
[17] H.Amemiya; Japan J.Appl.Phys., **27**, 694 **(1988)**.
[18] A.Savitzky, M.J.E.Golay; Anal.Chem., **36**, 1627 **(1964)**.
[19] V.Valdimir, Ivanov, S.Konstantin, Klopovsky, Dimitry Victorvitch Lopaev, A.Yurii A, Mankelevich, T.Alexander, Rakhimov, Tatyana V.Rakhimova; IEEE Transactions on Plasma Science, **31(4)**, 528 **(2003)**.
[20] A.J.Lichtenberg, V.Vahedi, M.A.Lieberman; J. Appl.Phys., **75(5)**, 2339 **(1993)**.
[21] R.W.B.Pearse, A.G.Gaydon; 'The Identification of Molecular Spectra', University Printing House Cambridge, **(1976)**.
[22] P.Krupenie; J.Phys.Chem.Ref.Data, **1**, 423 **(1972)**.
[23] M.A.Liberman, A.J.Lichtenberg; Principles of Plasma Discharges and Material Processing, John Willy & Sons, 223 **(1994)**.